

# Final state interactions in the electroweak nuclear response

Omar Benhar

INFN and Department of Physics, Università “La Sapienza”  
Piazzale Aldo Moro, 2. I-00185 Roma, Italy

I review the description of the electroweak nuclear response at large momentum transfer within nonrelativistic many-body theory. Special consideration is given to the effects of final state interactions, which are known to be large in both inclusive and semi-inclusive processes. The results of theoretical calculations of electron-nucleus scattering observables are compared to the data, and the generalization to charged current neutrino-nucleus interactions is discussed.

## 1. INTRODUCTION

Over the past few years the rapid development of neutrino physics, leading to significant improvements in the experimental accuracy, has triggered a burst of studies aimed at reducing the systematic uncertainty associated with the treatment of nuclear effects. The main results of these activities are discussed in the Proceedings of the previous meetings in the NUINT series [1,2].

It has soon been realized that much of the information needed to understand nuclear effects at quantitative level can be extracted from the large body of electron-nucleus scattering data [3], and that the theoretical techniques developed to describe the nuclear response to electromagnetic probes can be readily generalized to obtain accurate predictions of neutrino-nucleus scattering observables.

In this paper I review the approach based on nonrelativistic nuclear many-body theory (NMBT), that allows one to consistently include the effects of dynamical nucleon-nucleon (NN) correlations in both the initial and final states. The impulse approximation (IA) scheme, in which the cross section is written in terms of the nuclear spectral function  $P(p)$ , describing the momentum and energy distribution of nucleons in the target nucleus, is outlined in Section 2. Section 3 is devoted to the analysis of final state interactions (FSI), whose effects are known to be large, while in Section 4 the results of theoret-

ical calculations are discussed and compared to electron-nucleus scattering data. Finally, in Sections 5 I summarize the main results and state the conclusions.

## 2. THE IMPULSE APPROXIMATION

Let us consider the process

$$\ell + A \rightarrow \ell' + X, \quad (1)$$

in which  $\ell$  and  $\ell'$  denote either a charged lepton or a neutrino, and the final state of the target nucleus is unobserved. The corresponding differential cross section can be written in the form

$$\frac{d\sigma}{d\Omega_{\ell'} dE_{\ell'}} \propto L_{\mu\nu} W_A^{\mu\nu}, \quad (2)$$

where  $\Omega_{\ell'}$  and  $E_{\ell'}$  are the scattering angle and energy of the outgoing lepton, respectively. The tensor  $L_{\mu\nu}$  is totally specified by kinematics, whereas the definition of the target response tensor

$$W_A^{\mu\nu} = \sum_X \langle 0 | J_A^{\mu\dagger} | X \rangle \langle X | J_A^\nu | 0 \rangle \delta^{(4)}(p_0 + q - p_X), \quad (3)$$

involves the hadronic initial and final states  $|0\rangle$  and  $|X\rangle$ , carrying four-momenta  $p_0$  and  $p_X$ , respectively, as well as the nuclear electroweak current operator  $J_A^\mu$ .

Calculations of  $W_A^{\mu\nu}$  of Eq. (3) at moderate momentum transfer ( $|\mathbf{q}| < 0.5 \text{ GeV}$ ) can be carried out within NMBT, using nonrelativistic wave

functions and expanding the current operator in powers of  $|\mathbf{q}|/m$ , where  $m$  is the nucleon mass [5].

At higher momentum transfer, corresponding to beam energies larger than  $\sim 1$  GeV, describing the final states  $|X\rangle$  in terms of nonrelativistic nucleons is no longer possible. Due to the prohibitive difficulties involved in a fully consistent treatment of the relativistic nuclear many-body problem, calculations of  $W_A^{\mu\nu}$  in this regime require a set of simplifying assumptions, allowing one to take into account the relativistic motion of final state particles carrying momenta  $\sim \mathbf{q}$ , as well as the possible occurrence of inelastic processes leading to the appearance of hadrons other than protons and neutrons.

The main assumption underlying IA is that, as the space resolution of a probe delivering momentum  $\mathbf{q}$  is  $\sim 1/|\mathbf{q}|$ , at large enough  $|\mathbf{q}|$  the target is seen by the probe as a collection of individual nucleons. Hence, in the IA regime, the scattering process off a nuclear target reduces to the incoherent sum of elementary processes involving only one nucleon<sup>1</sup>.

The simplest implementation of IA, referred to as Plane Wave Impulse Approximation (PWIA) is based on the further assumption that the effects of FSI between the hit nucleon and the (A-1)-nucleon spectator system be negligible. The resulting picture of the scattering process is schematically illustrated in Fig. 1.

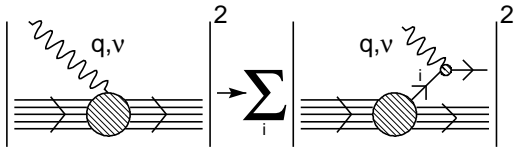


Figure 1. Pictorial representation of the PWIA scheme, in which the nuclear cross section is replaced by the incoherent sum of cross sections describing scattering off individual nucleons, the recoiling (A-1)-particle system acting as a spectator.

<sup>1</sup>Coherent contributions, not taken into account in the impulse approximation, play a role even at large  $|\mathbf{q}|$  for values of the Bjorken scaling variable  $x < 0.2$ , corresponding to very large lepton energy loss. However, they are not relevant to the kinematical regime discussed in this paper.

Within PWIA the target response tensor of Eq. (3) reduces to

$$W_A^{\mu\nu}(q) = \int d^4p P(p) \widetilde{W}^{\mu\nu}(p, q), \quad (4)$$

where  $q \equiv (\nu, \mathbf{q})$  is the four-momentum transfer. The nuclear spectral function  $P(p)$ , with  $p \equiv (M_A - E_{A-1}, \mathbf{p})$ , yields the probability of removing a nucleon with momentum  $\mathbf{p}$  from the target ground state leaving the residual system with energy  $E_{A-1}$  [6,7], whereas the tensor  $\widetilde{W}^{\mu\nu}$  describes the electroweak interactions of a *bound* nucleon. Within IA binding effects can be easily taken into account setting [8]

$$\widetilde{W}^{\mu\nu}(p, q) = W^{\mu\nu}(p, \tilde{q}), \quad (5)$$

where  $W^{\mu\nu}$  is the tensor associated with a *free* nucleon, that can be expressed in terms of the measured structure functions, and  $\tilde{q} \equiv (\tilde{\nu}, \mathbf{q})$ , with

$$\tilde{\nu} = \nu + M_A - E_{A-1} - \sqrt{|\mathbf{p}|^2 + m^2}. \quad (6)$$

According to Eqs. (5)-(6) a fraction  $(\nu - \tilde{\nu})/\nu$  of the lepton energy loss is spent to put the struck nucleon on the mass shell, and the elementary scattering process is described as if it took place in free space with energy transfer  $\tilde{\nu} < \nu$ .

While being fully justified on physics grounds, as part of the lepton energy loss does go into excitation energy of the spectator system, the replacement of  $\nu$  with  $\tilde{\nu}$  poses a non-trivial conceptual problem, in that it leads to a violation of vector current conservation. However, this issue turns out to be only marginally relevant, since the non gauge invariant contributions can be shown to vanish in the  $|\mathbf{q}| \rightarrow \infty$  limit.

### 3. FINAL STATE INTERACTIONS

The occurrence of strong FSI in quasi-elastic electron-nucleus scattering has long been experimentally established. One of the most striking evidences is the loss of flux of outgoing particles observed in electron induced proton knock-out experiments [9,10,11,12,13]. The suppression of the measured nuclear transparencies with respect to the PWIA limit turns out to be as strong as 20-40 % in Carbon and 50-70 % in Gold.

A theoretical description of FSI based on NMBT and a generalization of Glauber theory of high energy proton scattering [14] has been proposed in the early 90's [15]. This approach, generally referred to as Correlated Glauber Approximation (CGA), rests on the premises that i) the struck nucleon moves along a straight trajectory with constant velocity (eikonal approximation), and ii) the spectator nucleons are seen by the struck particle as a collection of fixed scattering centers (frozen approximation).

Under the above assumptions the propagator, describing the struck nucleon at time  $t$  after the electroweak interaction, can be written in the factorized form [16]

$$U_{\mathbf{p}+\mathbf{q}}(t) = U_{\mathbf{p}+\mathbf{q}}^0(t)\bar{U}_{\mathbf{p}+\mathbf{q}}^{FSI}(t), \quad (7)$$

where  $U_{\mathbf{p}+\mathbf{q}}^0(t)$  is the free space propagator, while FSI effects are described by the quantity

$$\bar{U}_{\mathbf{p}+\mathbf{q}}^{FSI}(t) = \langle 0|U_{\mathbf{p}+\mathbf{q}}^{FSI}(\mathbf{r}_1, \tilde{R}; t)|0\rangle. \quad (8)$$

Here  $\mathbf{r}_1$  and  $\tilde{R} \equiv (\mathbf{r}_2 \dots \mathbf{r}_A)$  specify the positions of the struck particle and the spectators, respectively,  $\langle 0|\dots|0\rangle$  denotes the expectation value in the target ground state and

$$U_{\mathbf{p}+\mathbf{q}}^{FSI}(\mathbf{r}_1, \tilde{R}; t) = e^{-i\sum_j \int_0^t dt' \Gamma_{\mathbf{p}+\mathbf{q}}(|\mathbf{r}_{1j} + \mathbf{v}t'|)}. \quad (9)$$

In Eq. (9),  $\mathbf{r}_{1j} = \mathbf{r}_1 - \mathbf{r}_j$  ( $j = 2, \dots, A$ ) and  $\Gamma_{\mathbf{p}+\mathbf{q}}(|\mathbf{r}|)$  is the coordinate-space  $t$ -matrix, simply related to the measured nucleon-nucleon (NN) scattering amplitude at incident momentum  $\mathbf{p} + \mathbf{q}$ . At large  $|\mathbf{q}|$ ,  $\mathbf{p} + \mathbf{q} \approx \mathbf{q}$  and the eikonal propagator of Eq. (8) becomes a function of  $t$  and the momentum transfer only.

The quantity

$$P_{\mathbf{q}}(t) = \langle 0||U_{\mathbf{q}}^{FSI}(\mathbf{r}_1, \tilde{R}; t)|^2|0\rangle \quad (10)$$

measures the probability that the struck nucleon do not undergo rescattering processes during a time  $t$  after the electroweak interaction. In absence of FSI, i.e. for vanishing  $\Gamma_{\mathbf{q}}$ ,  $P_{\mathbf{q}}(t) \equiv 1$ . Note that  $P(t)$  is trivially related to the nuclear transparency  $T_{\mathbf{q}}$ , measured in coincidence ( $e, e'p$ ) experiments [9,10,11,12,13], through

$$T_A = \lim_{t \rightarrow \infty} P_{\mathbf{q}}(t) \quad (11)$$

It is very important to realize that, as shown by Eqs. (8)-(10), the probability that a rescattering process occur is not simply dictated by the nuclear density distribution  $\rho_A(\mathbf{r}_j)$ , yielding the probability of finding a spectator at position  $\mathbf{r}_j$ . It depends upon the *joint* probability of finding the struck particle at position  $\mathbf{r}_1$  and a spectator at position  $\mathbf{r}_j$ , that can be written in the form

$$\rho^{(2)}(\mathbf{r}_1, \mathbf{r}_j) = \rho_A(\mathbf{r}_1)\rho_A(\mathbf{r}_j)g(\mathbf{r}_1, \mathbf{r}_j). \quad (12)$$

Due to the strongly repulsive nature of nuclear interactions at short range,  $\rho^{(2)}(\mathbf{r}_1, \mathbf{r}_j)$  is largely affected by NN correlations, whose effect is described by the correlation function  $g(\mathbf{r}_1, \mathbf{r}_j)$ . The results of numerical calculations carried out within NMBT yield  $g(\mathbf{r}_1, \mathbf{r}_j) \ll 1$  at  $|\mathbf{r}_{1j}| < 1$  fm.

The results displayed in Fig. 2 show that both the magnitude and the  $A$ - and  $Q^2$ -dependence of the transparencies of Carbon, Iron and Gold obtained from the approach of Ref. [15] are in good agreement with the experimental data. Note that in absence of FSI  $T_A(Q^2) \equiv 1$ .

The calculated nuclear transparencies turn out to be strongly affected by NN correlations. Neglecting their effects by setting  $g(\mathbf{r}_1, \mathbf{r}_j) \equiv 1$  in Eq. (12), one obtains  $T_A \approx 0.5$  and  $0.3$  for Carbon and Iron, respectively, at  $Q^2 > 2$ . Figure 2 shows that these values are utterly incompatible with the data.

Being only sensitive to rescattering processes taking place within a distance  $\sim 1/|\mathbf{q}|$  of the electroweak vertex, the inclusive cross section at high momentum transfer is much less affected by FSI than the ( $e, e'p$ ) cross section. However, FSI effects are appreciable, and become dominant in the low  $\nu$  tail, where PWIA calculations largely underestimate electron-nucleus scattering data.

In inclusive processes FSI have two effects: i) an energy shift of the cross section, due to the fact that the struck nucleon moves in the average potential generated by the spectator particles and ii) a redistribution of the strength, leading to the quenching of the quasielastic peak and the enhancement of the tails, as a consequence of the occurrence of NN scattering processes coupling the one particle-one hole final state to more complex  $n$ -particle  $n$ -hole configurations.

According to Ref. [15], in presence of FSI the

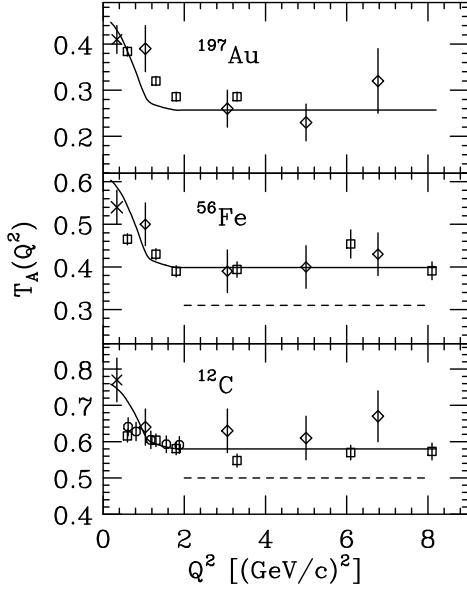


Figure 2.  $Q^2$ -dependence of the transparency of Carbon, Iron and Gold, calculated within the approach of Ref.[15]. The data points are taken from Refs.[9] (crosses), [10] (diamonds), [11,12] (squares) and [13] (circles). The dashed lines have been obtained neglecting the effect of NN correlations, i.e. setting  $g(\mathbf{r}_1, \mathbf{r}_j) \equiv 1$  in Eq. (12). Note that in absence of FSI  $T_A(Q^2) \equiv 1$ .

inclusive cross section can be expressed in terms of the PWIA result through

$$\frac{d\sigma}{d\Omega_{e'} d\nu} = \int d\nu' \left( \frac{d\sigma}{d\Omega_{e'} d\nu'} \right)_{PWIA} f_{\mathbf{q}}(\nu - \nu'), \quad (13)$$

the folding function  $f_{\mathbf{q}}(\nu)$  being defined as

$$f_{\mathbf{q}}(\nu) = \delta(\nu) \sqrt{T_A} + \int \frac{dt}{2\pi} e^{i\nu t} \left[ \bar{U}_{\mathbf{q}}^{FSI}(t) - \sqrt{T_A} \right]. \quad (14)$$

The above equations clearly show that the strength of FSI is measured by both  $T_A$  and the width of the folding function. In absence of FSI,  $\bar{U}_{\mathbf{q}}^{FSI}(t) \equiv 1$ , implying in turn  $T_A = 1$  and  $f_{\mathbf{q}}(\nu) \rightarrow \delta(\nu)$ .

#### 4. RESULTS

The approach described in the previous Sections has been employed to carry out calculations of the inclusive cross sections for both

electron-nucleus and charged current neutrino-nucleus processes.

In Fig. 3 the cross section of the process  $e + {}^{16}\text{O} \rightarrow e' + X$ , obtained from Eq. (13) [4], is compared to the data of Ref. [17]. The results of theoretical calculation, *involving no adjustable parameters*, provide a very accurate description of the measured cross sections in the region of the quasi-elastic peak. The effect of FSI, leading to a shift and a quenching of the peak, is clearly visible. For reference, the figure also shows the results of the Fermi gas (FG) model, corresponding to Fermi momentum  $p_F = 225$  MeV and nucleon removal energy  $\epsilon = 25$  MeV, which appears to largely overestimate the data. The failure of the theoretical calculations to reproduce the measured cross section in the region of the  $\Delta$ -production peak is likely to be ascribable to deficiencies in the description of the elementary electron-nucleon cross section [4].

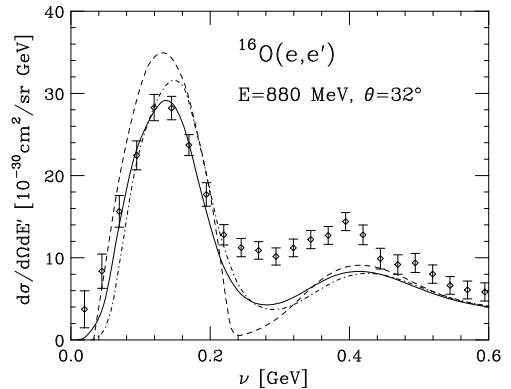


Figure 3. Cross section of the process  ${}^{16}\text{O}(e, e')$  at beam energy 880 MeV and electron scattering angle  $32^\circ$ . Solid line: full calculation. Dot-dash line: PWIA calculation, carried out neglecting FSI effects. Dashed line: FG model with  $p_F = 225$  MeV and  $\epsilon = 25$  MeV. The experimental data are from Ref.[17].

In Figs. 4 and 5 the results of the approach of Ref. [15] are compared to the cross section at beam energy  $E_e = 3.6$  GeV and scattering angle  $\theta_{e'} = 30^\circ$  (corresponding to  $Q^2 \gtrsim 2$  GeV<sup>2</sup>) obtained from the extrapolation of SLAC ( $e, e'$ ) data to infinite  $A$  [18].

Figure 4 clearly shows the dominance of FSI in the low energy loss tail of the cross section, as well as the need of including of NN correlations to achieve a quantitative account of the data.

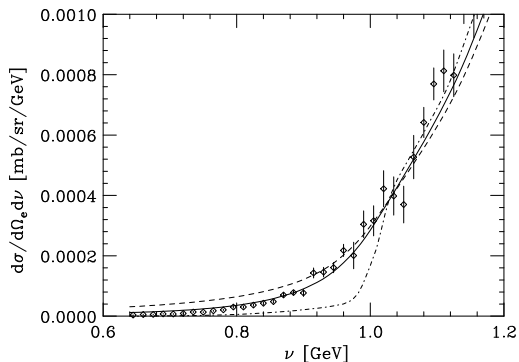


Figure 4. Comparison between the results of the approach of Ref. [15] and the extrapolated nuclear matter cross section of Ref. [18] at  $E_e = 3.6$  GeV and  $\theta_{e'} = 30^\circ$ . Dash-dot line: PWIA calculation. Solid line: full calculation, including FSI. The dashed line has been obtained neglecting the effects of NN correlations in the calculation of FSI effects, i.e. setting  $g(\mathbf{r}_1, \mathbf{r}_j) \equiv 1$  in Eq. (12).

The data displayed in Fig. 5 show that the transition from the quasi elastic to the inelastic regime, including resonant and nonresonant pion production as well as deep inelastic processes, is a smooth one, thus suggesting the possibility of a unified theoretical representation. It appears that NMBT and the IA scheme provide a consistent and computationally viable approach, yielding a good description of the measured cross section over the whole  $\nu$  range.

The energy loss spectra obtained applying the formalism discussed in the previous Sections to charged current neutrino-nucleus scattering exhibit qualitative features similar to those emerging from the analysis of electron-nucleus scattering [4].

The effect of Pauli blocking of the phase space available to the knocked-out particle, while being hardly visible in Figs. 3-5, is large in the  $Q^2$  distributions at  $Q^2 < 0.2$  GeV<sup>2</sup>. This feature is illustrated in Fig. 6, showing the calculated differential cross section  $d\sigma/dQ^2$  of the process

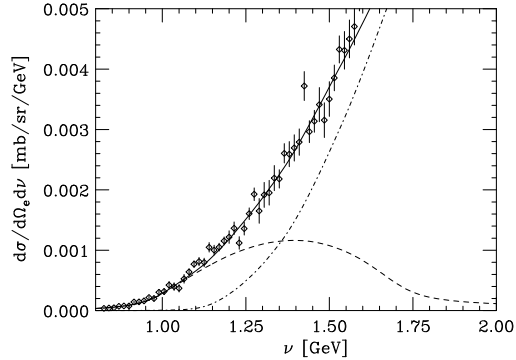


Figure 5. Comparison between the results of the approach of Ref. [15] and the extrapolated nuclear matter cross section of Ref. [18] at  $E_e = 3.6$  GeV and  $\theta_{e'} = 30^\circ$ . Dashed line: contribution of quasielastic scattering. Dash-dot line: contribution of inelastic channels. Solid line: full calculation.

$\nu_e + {}^{16}\text{O} \rightarrow e + X$ , for neutrino energy  $E_\nu = 1$  GeV [4]. The dashed and dot-dash lines correspond to the PWIA results with and without inclusion of Pauli blocking, respectively. It clearly appears that the effect of Fermi statistics in suppressing scattering shows up at  $Q^2 < 0.2$  GeV<sup>2</sup> and becomes very large at lower  $Q^2$ . The results of the full calculation, in which dynamical FSI are also included, are displayed as a full line.

Figure 6 suggests that Pauli blocking and FSI may explain the deficit of the measured cross section at low  $Q^2$  with respect to the predictions of Monte Carlo simulations [19].

## 5. CONCLUSIONS

The results discussed in this paper show that the approach based on NMBT provides quantitative *parameter free* predictions of the electroweak nuclear response in the impulse approximation regime, corresponding to beam energy larger than  $\sim 1$  GeV, relevant to many neutrino oscillation experiments.

In the region of the quasi-elastic peak, theoretical results account for the measured  ${}^{16}\text{O}(e, e')$  cross sections at beam energies between 700 MeV and 1200 MeV and scattering angle  $32^\circ$  with an accuracy better than 10 % [4]. Close agreement between theory and data is also found at larger

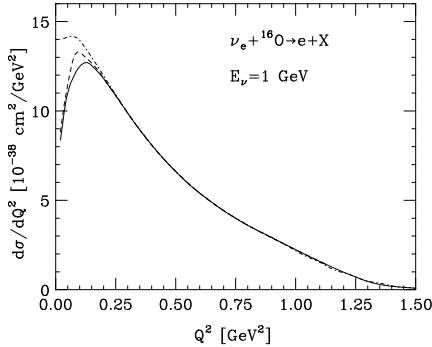


Figure 6. Differential cross section  $d\sigma/dQ^2$  for neutrino energy  $E_\nu = 1$  GeV. The dot-dash line shows the PWIA results, while the solid and dashed lines have been obtained taking into account the effect of Pauli blocking, with and without inclusion of dynamical FSI, respectively.

energies, where inelastic processes dominate, with the only exception of the region of quasi-free  $\Delta$  production, where theoretical predictions significantly underestimate the measured cross sections. Although the disagreement is likely to be ascribable to uncertainties in the description of the nucleon structure functions at low  $Q^2$ , further studies are needed to clarify this issue.

The overall picture emerging from the comparison between theory and electron scattering data indicates that FSI are large and *do not* go away at large  $Q^2$ , as the total NN cross section, dominated by inelastic contributions, stays roughly constant over a broad energy range [20]. The main FSI effects in both inclusive and semi-inclusive processes appear to be understood. The pivotal role played by NN correlation entails that a fully quantitative treatment of FSI requires a realistic description of nuclear dynamics beyond the mean field approximation.

## ACKNOWLEDGMENTS

The results discussed in this paper have been obtained in collaboration with N. Farina, H. Nakamura, D. Rohe, M. Sakuda, R. Seki and I. Sick. A number of illuminating discussions with A. Fabrocini, S. Fantoni and R. Schiavilla are also gratefully acknowledged.

## REFERENCES

1. Proceedings of the First International Workshop on Neutrino-Nucleus Interactions in the Few GeV Region, Eds. J.G. Morfin, M. Sakuda and Y. Suzuki. Nucl. Phys. B (Proc. Suppl.) 112 (2002).
2. Proceedings of the Third International Workshop on Neutrino-Nucleus Interactions in the Few GeV Region, Eds. F. Cavanna, P. Lipari, C. Keppel and M. Sakuda. Nucl. Phys. B (Proc. Suppl.) 139 (2005).
3. *Electron Nucleus Scattering VII*, Eds. O. Benhar, A. Fabrocini, S. Fantoni and R. Schiavilla, Eur. Phys. J. A 17 (2003).
4. O. Benhar, N. Farina, H. Nakamura, M. Sakuda and R. Seki, Phys. Rev. D 72 (2005) 053005.
5. J. Carlson and R. Schiavilla, Rev. Mod. Phys. 70 (1998) 743.
6. O. Benhar, A. Fabrocini and S. Fantoni, Nucl. Phys. A505 (1989) 267.
7. O. Benhar, A. Fabrocini, S. Fantoni and I. Sick, Nucl. Phys. A579 (1994) 493.
8. T. de Forest, Jr., Nucl. Phys. A392 (1983) 232.
9. G. Garino *et al*, Phys. Rev. C 45 (1992) 78.
10. T.G. O'Neill *et al*, Phys. Lett. B351 (1995) 87.
11. D. Abbott *et al*, Phys. Rev. Lett. 80 (1998) 5072.
12. K. Garrow *et al*, Phys. Rev. C 66 (2002) 044613.
13. D. Rohe *et al*, Phys. Rev. C 72 (2005) 054602.
14. R.J. Glauber, Lect. in Theor. Phys., Eds. W.E. Brittin *et al*. (Interscience, New York, 1959).
15. O. Benhar *et al*, Phys. Rev. C 44 (1991) 2328.
16. M. Petraki *et al*, Phys. Rev. C 67 (2003) 014605.
17. M. Anghinolfi *et al.*, Nucl. Phys. A602 (1996) 405.
18. B.D. Day *et al.*, Phys. Rev. C 40 (1989) 1011.
19. T. Ishida, Nucl. Phys. B Proc. Suppl., 112 (2002) 132.
20. O. Benhar, Phys. Rev. Lett. 83 (1999) 3130.